MARVELD1 attenuates arsenic trioxide-induced apoptosis in liver cancer cells by inhibiting reactive oxygen species production

Wenping Ma[1], Haiyang Shen[2], Qian Li[2], Hao Song[2], Yanyan Guo[2], Fangrong Li[2], Xingang Zhou[3], Xinwu Guo[4], Jingdong Shi[5], Qi Cui[1], Jinhao Xing[1], Jinhai Deng[6], Youtao Yu[2], Wenjie Liu[7], Hongshan Zhao[1]

[1]Department of Medical Genetics, School of Basic Medical Sciences, Peking University Health Science Center, Beijing 100191, China; [2]Department of Intervention Therapy, The Fourth Medical Center of PLA General Hospital, Beijing 100048, China; [3]Department of Pathology, Beijing Ditan Hospital, Capital Medical University, Beijing 100015, China; [4]Sansure Biotech Inc., Changsha 410205, China; [5]Department of General Surgery, Beijing Tiantan Hospital, Capital Medical University, Beijing 100070, China; [6]Department of Immunology, School of Basic Medical Sciences, Peking University Health Science Center, Beijing 100191, China; [7]Department of Hepatobiliary Surgery, National Cancer Center/Cancer Hospital, Chinese Academy of Medical Sciences and Peking Union Medical College, Beijing 100021, China

Contributions: (I) Conception and design: W Ma, Y Yu, W Liu, H Zhao; (II) Administrative support: Y Yu; (III) Provision of study materials or patients: Y Yu; (IV) Collection and assembly of data: W Ma, H Shen, X Zhou, Q Cui, H Zhao; (V) Data analysis and interpretation: W Ma, Q Li, H Song, Y Guo, F Li, X Guo, J Shi, J Xing, J Deng, W Liu; (VI) Manuscript writing: All authors; (VII) Final approval of manuscript: All authors.

Correspondence to: Youtao Yu. Department of Intervention Therapy, The Fourth Medical Center of PLA General Hospital, Beijing 100048, China. Email: yuyoutao@126.com; Wenjie Liu. Department of Hepatobiliary Surgery, National Cancer Center/Cancer Hospital, Chinese Academy of Medical Sciences and Peking Union Medical College, Beijing 100021, China. Email: wenjie6363@163.com; Hongshan Zhao. Department of Medical Genetics, School of Basic Medical Sciences, Peking University Health Science Center, Beijing 100191, China. Email: hongshan@bjmu.edu.cn.

Background: Arsenic trioxide (As_2O_3) is widely used for the treatment of acute promyelocytic leukemia (APL), and more recently, has also been applied to solid tumors. However, there are a fraction of patients with solid tumors, such as liver cancer, who respond to As_2O_3 treatment poorly. The underlying mechanisms for this remain unclear.

Methods: We determined the suitable concentration of drugs by IC50. Cell Counting Kit-8 (CCK-8) and flow cytometry were used to analyze the apoptosis. Morphological changes of the cells were observed by laser scanning confocal microscopy. Furthermore, reactive oxygen species (ROS) and mitochondrial membrane potential (MMP) were detected by flow cytometry. Quantitative polymerase chain reaction (qPCR) and Western blot tests were conducted to detect the mRNA and protein levels in different groups. Finally, a xenograft tumor assay and histopathological analysis were performed to evaluate the MARVELD1 function in cell proliferation and apoptosis.

Results: Here, we show that MARVELD1 enhances the therapeutic effects of epirubicin, while inducing the strong resistance of liver cancer cells to As_2O_3 treatment. We further demonstrate that the As_2O_3-induced apoptosis was inhibited by MARVELD1 overexpression (24 h Vector *vs.* MARVELD1 =30.58% *vs.* 17.41%, P<0.01; 48 h Vector *vs.* MARVELD1 =46.50% *vs.* 21.02%, P<0.01), possibly through inhibiting ROS production by enhancing TRXR1 expression. *In vivo*, we found a significantly increased size (Vector *vs.* MARVELD1 =203.90±21.92 *vs.* 675.70±37.84 mm^3, P<0.001) and weight (Vector *vs.* MARVELD1 =0.19±0.02 *vs.* 0.58±0.05 g, P<0.001) of tumors with high expression of MARVELD1 after As_2O_3 treatment. Consistently, a higher expression of MARVELD1 predicted a poor prognosis for liver cancer patients.

Conclusions: Our data identified a unique role of MARVELD1 in As_2O_3-induced apoptosis and As_2O_3 cancer therapy resistance.

Keywords: Arsenic trioxide (As_2O_3); MARVELD1; apoptosis; therapy; reactive oxygen species (ROS)

Submitted Jan 14, 2019. Accepted for publication Apr 07, 2019.

doi: 10.21037/atm.2019.04.38

View this article at: http://dx.doi.org/10.21037/atm.2019.04.38

Introduction

Hepatocellular carcinoma (HCC) is one of the most common malignant liver tumors in the world (1). The current standard treatment for HCC includes surgical resection, drug treatment, and liver transplantation (1-4); however, all these treatments are less than satisfactory due to the liver's abundant blood supply, intra-hepatic and extra-hepatic metastasis, post-surgical tumor recurrence, and drug resistance (5). Understanding and avoiding drug resistance are urgently needed for the benefits of HCC patients.

Arsenic trioxide (As_2O_3) is an effective chemotherapeutic agent for acute promyelocytic leukemia (APL) and other hematopoietic malignancies (6). Recently, more evidence has demonstrated its therapeutic potential in solid tumors (7). Studies show that As_2O_3 reduced the migration and angiogenesis by targeting FOXO3a in gastric cancer cells (8). It was reported that As_2O_3 inhibited prostate cancer cell viability and induced apoptosis through the Wnt signal pathway (9). However, the clinical application of As_2O_3 in HCC is hindered by its high toxicity and acquired drug resistance.

MARVELD1 (*MARVEL* domain-containing 1) is one of the *MARVEL* genes that is related to MAL and related proteins for vesicle trafficking and membrane links. Its domain-containing proteins are believed to be tumor suppressor genes, which are frequently downregulated via promoter methylation in breast, cervical, prostate, hepatocellular, esophageal, and gastric carcinoma or cell lines (10-12). MARVELD1 has been shown to inhibit cell proliferation and enhance chemo-sensitivity to epirubicin and 10-hydroxycamptothecin in HCC cell lines (13). However, the role of MARVELD1 in the treatment response of HCC to As_2O_3. remains unknown. Here, we found that HepG2 cells which were stably expressing MARVELD1 showed a lower apoptosis rate in response to the As_2O_3 treatment. Similar results were observed in a transient overexpression experiment. We further showed that reactive oxygen species (ROS) induction by As_2O_3 treatment was significantly inhibited by the overexpression of MARVELD1. Consistently, cancer cells with overexpressed MARVELD1 grew more vigorously in response to As_2O_3 treatment. Our findings may help predict the prognosis of patients with HCC receiving As_2O_3 therapy.

Methods

Reagents

All reagents were of analytical grade. Milli-Q water (Millipore) was used throughout the experiment. Arsenious acid and sodium chloride injections (10 mg/mL) were purchased from the Pharmaceutical Limited of Harbin Medical University. Epirubicin was purchased from Selleck Chemicals. The Cell Counting Kit-8 (CCK-8) and Oxygen Species Assay Kit were purchased from the Beijing Solarbio Science & Technology Co. The Mitochondrial Membrane Potential (MMP) Assay Kit was purchased from Beijing Beyotime Biotechnology. Fetal bovine serum (FBS) was purchased from HYCLONE. RPMI 1640 was purchased from Gibco. Lipofectamine™ 3000 Transfection Reagent leverages was purchased from Invitrogen. Colorimetric TUNEL Apoptosis Assay Kit (C1091) was purchased from Beyotime Biotechnology.

Antibodies

Antibodies against MARVELD1 (ab91640) and Ki67 (ab15580) were bought from Abcam. Caspase-3 [9662], PARP-1 [9532], TRXR1 [15140], BCL-2 [15071], and BAX [14796] antibodies were bought from CST. GAPDH (AF7021) antibodies were purchased from Affinity Biosciences.

Cell culture

The MARVELD1 plasmid, HepG2-vector-, and HepG2-MARVELD1-stably-transfected cell lines were gifts from the School of Life Science and Technology of the Harbin Institute of Technology. HepG2 and PLC/PRF/5 cells were purchased from ATCC. All cells were cultured in Gibco™ RPMI 1640 medium with 10% FBS and grown in a medium supplemented with 100 units per mL penicillin and 100 mg per mL streptomycin at 37 ℃ and 5% CO_2. After 24 hours of incubation, the supernatant was discarded, the cell cultures were washed with phosphate buffered saline (PBS) three times, and fresh medium was added with the indicated doses of As_2O_3 for the indicated time.

IC50 test and cell viability assay

First, we determined the suitable concentration of drugs. HepG2 cells were seeded into 96-well plates (2×10^3 cells/well). After 24 hours of incubation, the cells were then treated with different doses of As_2O_3 ranging from 0 to 200 μM. After 48 hours of treatment, 10 μL of CCK-8 were added to each well and incubated for two hours. The data was then obtained using a Bio-Rad microplate reader

(Bio-Rad, Hercules, CA, USA). Cell viability was calculated using the following formula: cell viability (%) = [(A450 of test group-A450 of the blank group)]/[(A450 of the control group-A450 of the blank group)] ×100.

IC50 was obtained via probit analysis and calculated using GraphPad Prism 6.0 software. IC50 was measured in duplicates, and each experiment was repeated three times.

Annexin V/propidium iodide (PI) assays for apoptosis

For the annexin V/PI assays, cells were dual-stained with annexin V-FITC and PI, and then subsequently evaluated for early and late apoptosis using flow cytometry, as per the manufacturer's instructions (14,15). HepG2-Vector and HepG2-MARVELD1 were treated with As_2O_3 (20 μM) for 48 hours, harvested, and washed twice with PBS. The cells were then stained with 10 μL of annexin V-FITC for 30 minutes, and then 5 μL of PI for 5 minutes in the dark at room temperature, in 100 μL of binding buffer, before undergoing flow cytometry. Briefly, 1×10^4 cells were detected and analyzed using BD FACS Calibur™ software (BD Biosciences, Franklin Lakes, NJ, USA). Data were shown as early apoptosis and late apoptosis in the MARVELD1 group compared to the vector group.

Measurement of intracellular (reactive oxygen species) ROS

The two cell groups were seeded into 6-well culture plates for 24 hours and were exposed to 20 μM of As_2O_3 or PBS for 24 hours at 37 ℃. The cells were then harvested, resuspended in fresh culture medium containing 10 mM dichloro-dihydro-fluorescein diacetate (DCFH-DA), and incubated in a 37 ℃ water bath for 30 minutes. The formation of fluorescent-oxidized DCF was monitored using a FACS Calibur flow cytometer (excitation at 485 nm, emission at 535 nm). The generated ROS was quantified by evaluating the fluorescence intensity of 1×10^4 cells using a BD FACS Calibur™.

MMP assay

The changes in MMP (ΔΨm) were monitored using rhodamine 123 2-(6-Amino-3-imino-3H-xanthen-9-yl) benzoic acid methyl ester. The two cell groups were seeded into 6-well culture plates for 24 hours and were exposed to 20 μM of As_2O_3 or PBS for 24 hours at 37 ℃. The cells were then stained with rhodamine 123 (1 μM) and kept in the dark at 37 ℃ for 20 minutes (16). Later, the cells were washed twice with PBS and immediately analyzed by flow cytometry using a BD FACS Calibur™.

Laser scanning confocal microscopy

Morphological changes of the cells were observed using Hoechst 33342 staining. Apoptotic cells will generally display condensed DNA and fragmented nuclei (17,18). Cells were seeded into 6-well culture plates for 24 hours and exposed to 20 μM of As_2O_3 or PBS for 24 hours at 37°C. Cold 1× PBS was used to wash cells three times for 5 minutes each time. Cells were then fixed with a 4% formaldehyde solution for 20–30 minutes at room temperature. 1× PBS was used to wash the cells three times, for 5 minutes each time. Cells underwent permeation for 5 minutes at room temperature using 0.2% Triton X-100. Cells were washed three times with 1× PBS, for 5 minutes each time, and blocked with a 5% bovine serum albumin (BSA) for 30 minutes at room temperature. Cells were treated with a rabbit polyclonal MARVELD1 antibody (1:200 dilution with 1% BSA) in a wet box at 4 ℃ overnight. After washing with 1× PBS three times, for 5 minutes each time, secondary antibody (diluted with 1% BSA) was added to the cells and incubated for two hours in the dark. Cells were washed again with 1× PBS three times, for 5 minutes each time, and then incubated with Hoechst 33342 for 5 minutes. Cells were washed three times with 1× PBS, for 5 minutes each time, and mounted to slides using glycerol. The morphological changes in the nucleus caused by As_2O_3 in HepG2 cells were observed using a fluorescence microscope (DMI 4000 B, Leica, Germany). Cells with chromatin condensation and nuclear fragmentation were noted as hallmarks of apoptosis (18,19).

Western blot analysis

Cells were lysed in lysis buffer in the presence of a protease inhibitor cocktail (100X). Protein concentrations were determined by the Bio-Rad microprotein assay using a standard BSA kit. The whole cell protein lysates were separated using sodium dodecyl sulfate-polyacrylamide gel electrophoresis (SDS-PAGE) and blotted onto nitrocellulose (NC) transfer membranes. These membranes were then blocked using 5% non-fat milk and incubated with the relevant primary antibodies overnight at 4 ℃. Afterward, the membranes were washed twice with Tris-buffered saline with Tween 20 (TBST) and incubated with secondary antibodies (ZSGB Beijing, China) for one hour at room temperature.

After incubation, blots were assessed using an enhanced chemiluminescence detection device (GE).

Quantitative real-time polymerase chain reaction (qPCR)

Total cellular ribonucleic acid (RNA) was isolated using Trizol (Invitrogen, Carlsbad, CA, USA) according to the manufacturer's recommendations. For the detection of MARVELD1 and glyceraldehyde 3-phosphate dehydrogenase (GAPDH), total RNA (1 μg) was reverse-transcribed into complementary deoxyribonucleic acid (cDNA) using Takara reverse transcriptase. The primers used were synthesized by Sangon Co. (Shanghai, China) and the sequences were as follows: MARVELD1-F, 5'-GCTAGTCGCAGTGGCTCATG-3'; MARVELD1-R, 5'- GTGTGACCAGCTCT GGGAATC-3'; GAPDH-F, 5'- ACAACTTTGGTATCGTGGAAGG-3'; and GAPDH-R, 5'-GCCATCACGCCACAGTTTC-3'. RT-PCR was performed using the Applied Biosystems 7300 HT machine and Maxima TM SYBR Green/ROX qPCR Master Mix (Fermentas, Waltham, MA, USA). The PCR reaction was evaluated using melting curve analysis. GAPDH was used as an internal control. GAPDH was amplified to ensure cDNA integrity and to normalize expression. Fold-changes in the expression of each gene were calculated by a comparative threshold cycle (Ct) method using the formula, $2^{-(\Delta\Delta Ct)}$. Analyses for all samples were repeated three times.

Animal experiments

BALB/c nude mice were purchased from Beijing Vital River Laboratory Animal Technology Co., Ltd, and maintained in specific pathogen-free (SPF) animal facilities at room temperature with a 24-h night-day cycle and fed with pellets and water *ad libitum*. All procedures followed the Peking University Guidelines for using animals in intramural research and were approved by the Animal Care and Use Committee of Peking University. For the Xenograft tumor assay, log growth-phase of HepG2-MARVELD1 stable cells and control cells (1×10^6 cells in 0.1 mL PBS) were injected subcutaneously into the right flank of athymic nude mice. Tumor growth was observed every 3 days by measuring its diameter with Vernier calipers. Tumor volume = 1/2ab2 ("a" is the long diameter and "b" is the short diameter) (20). As_2O_3 (10 mg/kg) was intraperitoneally injected daily starting at three days post cell seeding. Mice were sacrificed using cervical dislocation when the tumor size reached about 2.0 cm in diameter or greater than 10% body weight, and the samples were collected.

Histopathological analysis

Tissues were paraffin-embedded, sectioned (thickness: about 4–5 μm), subjected to hematoxylin and eosin (HE) staining, and observed under a light microscope (×200 magnification) to study morphology. Immunohistochemistry (IHC) staining was performed to study cell proliferation and apoptosis.

Statistical analysis

Results were analyzed using the GraphPad Prism 6 software. All values were expressed as the mean ± SD. Data were statistically analyzed by unpaired 2 sample *t*-test and $P<0.05$, $P<0.01$, $P<0.001$ were considered statistically significant.

Results

MARVELD1 plays a different role in epirubicin- and As_2O_3-induced cytotoxicity

To test the effects of MARVELD1 on As_2O_3 treatment in a liver cancer cell line, we first determined the IC50 value using a previously established HepG2 cell line which stably expresses MARVELD1 (*Figure S1*). We used epirubicin treatment as control (Vector 82.71±0.08 μM *vs.* MARVELD1 51.97±0.14 μM, $P<0.001$, *Figure 1A*) and found that in contrast to Epirubicin, As_2O_3-treated HepG2-MARVELD1 stable cells showed significantly higher IC50 value (Vector 22.74±0.04 *vs.* MARVELD1 54.38±0.08 μM, $P<0.001$, *Figure 1B*), indicating resistance to As_2O_3 treatment. We then tested cell viability after different concentrations of As_2O_3 treatment and found 20uM was optimal (*Figure 1C*). This concentration was then used in the following experiment.

MARVELD1 inhibits As_2O_3 induced apoptosis in liver cancer cells

To explore the mechanisms underlying the As_2O_3 resistance, we first investigated the effects of As_2O_3 treatment on cell morphology. The HepG2-MARVELD1 stable cells showed less significant shrinkage and pyknosis under light microscopy after As_2O_3 treatment (*Figure 2A*), and chromatin condensation was also less severe in the HepG2-

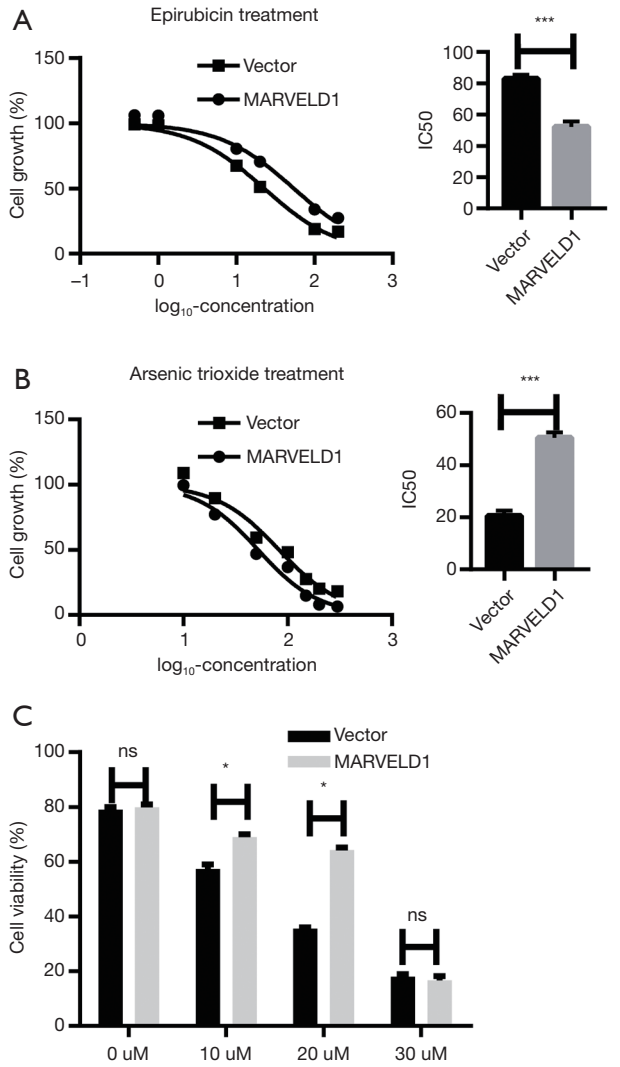

Figure 1 MARVELD1 shows different effects on As_2O_3 and epirubicin treatment in HepG2 cells. (A) Left, inhibition curve of epirubicin to determine IC50 in HepG2-MARVELD1 stable cells; right, comparison of IC50 between HepG2-MARVELD1 stable cells and control cells. (B) Left, inhibition curve of As_2O_3 to determine IC50 in HepG2-MARVELD1 stable cells; right, comparison of IC50 between HepG2-MARVELD1 stable cells and control cells. (C) Cell viability under different As_2O_3 concentrations treatment of HepG2-MARVELD1 stable cells and control cells for 48 hours. Data were pooled from at least three independent experiments. *, P<0.05; ***, P<0.001.

MARVELD1 stable cells (Vector 23.0±3.0 *vs.* MARVELD1 9.0±1.0, P<0.01, *Figure 2B*). To further confirm these findings, we next determined the apoptosis level of the different liver cancer cell lines treated with As_2O_3 for different time durations using flow cytometry. HepG2-MARVELD1 stable cells showed less apoptosis at both time points (24 h Vector *vs.* MARVELD1 =30.58% *vs.* 17.41%, P<0.01, *Figure 2C* upper); (48 h Vector *vs.* MARVELD1 =46.50% *vs.*21.02%, P<0.01, *Figure 2C* lower). HepG2 cells transiently transfected with MARVELD1 also showed less apoptosis after As_2O_3 treatment for 24 hours (Vector *vs.* MARVELD1 =50.33% *vs.* 21.02%, P<0.05, *Figure S2A*). PLC/PRF/5 cells showed a similar result (Vector *vs.* MARVELD1 =44.12% *vs.* 20.48%, P<0.05, *Figure S2B*). Consistently, As_2O_3 treatment induced less PARP-1, Caspase 3 cleavage, increased Bcl-2 expression, and decreased BAX expression in MARVELD1 overexpressed liver cancer cells (*Figure 2D*). Collectively, these data points indicate that MARVELD1 overexpression inhibited As_2O_3-induced apoptosis in liver cancer cells.

MARVELD1 inhibits ROS induction by As_2O_3 treatment through enhancing TRXR1 expression

Arsenic trioxide-induced cell death was mediated by the elevated production of ROS and mitochondrial damage (21). Therefore, we next investigated the effects of MARVELD1 overexpression on ROS production and MMP. We found that MARVELD1 overexpression significantly inhibited the production of ROS (Vector 11.4 to 69.2 *vs.* MARVELD1 9.2 to 15.4, P<0.01, *Figure 3A*) and the loss of MMP (Vector *vs.* MARVELD1 =94.98% *vs.* 57.91, P<0.01, *Figure 3B*). The thioredoxin (Trx) system is composed of thioredoxin reductase (TrxR), Trx, and NADPH, and it plays important roles in the regulation of the cellular redox environment (22). Arsenic trioxide has been shown to exert its effect mainly through inhibiting TrxR (23). We then further explored the effects of MARVELD1 overexpression on TRXR1 expression. We found strong resistance of TRXR1 to As_2O_3 inhibition in HepG2-MARVELD1 stable cells compared to control cells at both the mRNA level (*Figure 3C* and *Figure S3*) and protein level (*Figure 3D*). Thus, MARVELD1 inhibits ROS induction through enhancing TRXR1 expression.

MARVELD1 induces As_2O_3 resistance of liver cancer cells in vivo

To validate the importance of MARVELD1 overexpression for As_2O_3 resistance of liver cancer cells, we injected HepG2-MARVELD1 stable cells and control cells into nude mice. Liver cancer cells with a high expression of MARVELD1 formed more tumors with a larger size (Vector

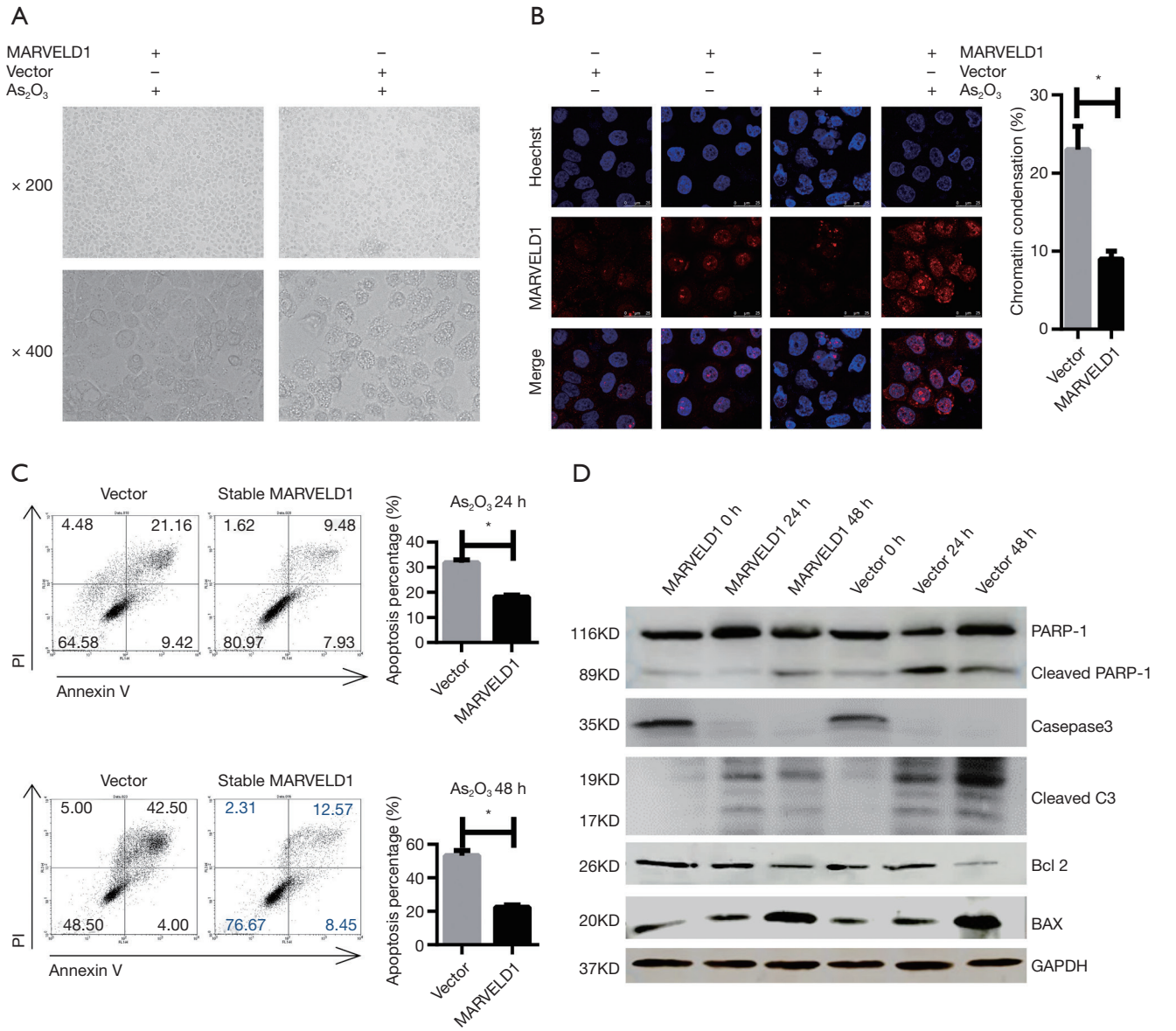

Figure 2 Overexpression of MARVELD1 leads to less apoptosis in HepG2 cells treated with As_2O_3. (A) Representative light microscopic images of HepG2-MARVELD1 stable cells and control cells treated with As_2O_3 for 24 hours. (B) Left, representative immunofluorescence images of HepG2-MARVELD1 stable cells and control cells treated with As_2O_3 for 24 hours; right, quantification of chromatin condensation. (C) Flow cytometry analysis of apoptosis of HepG2-MARVELD1 stable cells and control cells treated with As_2O_3 for a different time. (D) Immunoblotting of indicated proteins in HepG2-MARVELD1 stable cells and control cells treated with As_2O_3 for a different time. Data were pooled from at least three independent experiments. *, P<0.05.

vs. MARVELD1 =203.90±21.92 *vs.* 675.70±37.84 mm^3, P<0.001, *Figure 4A*) and weight (Vector *vs.* MARVELD1 =0.19±0.02 *vs.* 0.58±0.05 g, P<0.001, *Figure 4A*). Moreover, histological and immunohistochemical staining indicated more robust proliferation (Vector *vs.* MARVELD1 =0.09±0.01 *vs.* 0.74±0.01, P<0.001, *Figure 4A*) and less apoptosis in the tumors formed by HepG2-MARVELD1 stable cells (Vector *vs.* MARVELD1 =0.61±0.04 *vs.* 0.13±0.02, P<0.001, *Figure 4B*). A previous report showed a reduction of MARVELD1 expression in liver cancer tissue compared to peri-cancer tissue. However, it is worth noting that the expression level of MARVELD1

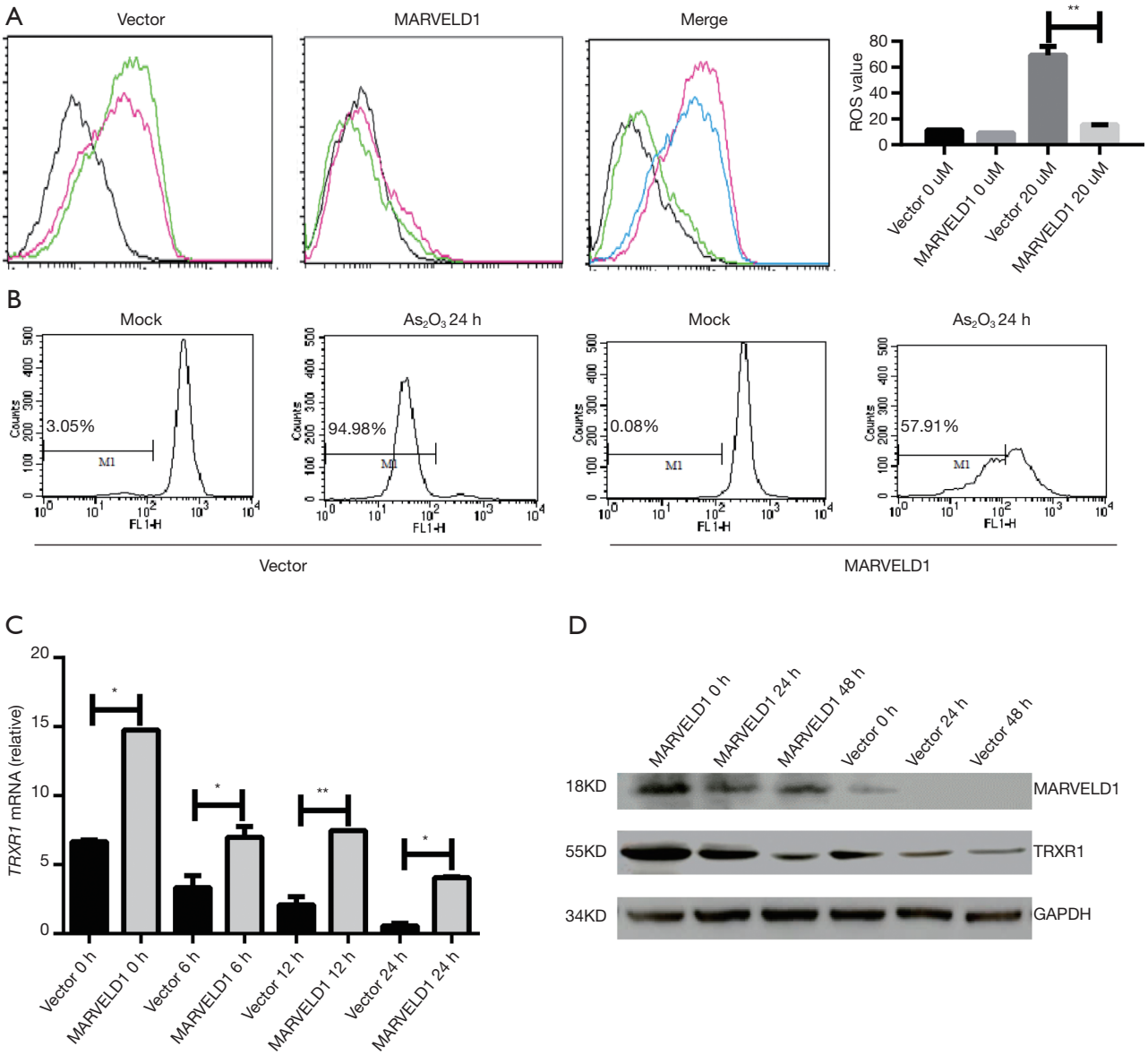

Figure 3 MARVELD1 inhibits ROS production by promoting TRXR1 expression. (A) Flow cytometry analysis of ROS level in HepG2-MAEVELD1 stable cells and control cells treated with As_2O_3. (B) Flow cytometry analysis of mitochondrial membrane potential in HepG2-MAEVELD1 stable cells and control cells treated with As_2O_3. (C) Time course of TRXR1 mRNA level change in HepG2-MAEVELD1 stable cells and control cells treated with As_2O_3. (D) Immunoblotting of indicated proteins in HepG2-MAEVELD1 stable cells and control cells treated with As_2O_3 for the different time. Data were pooled from at least three independent experiments. *, P<0.05. **, P<0.01. ROS, reactive oxygen species.

in cancer tissue varied among the patients (12), and we also confirmed this result (*Figure S4*). More interestingly, we noticed that a higher expression of MARVELD1 was significantly related to the worse overall survival of liver cancer patients (P=0.045, *Figure 4C*) (24). Taken together, our study strongly suggests a crucial role that MARVELD1plays in the resistance of liver cancer for As_2O_3 treatment and the pathogenesis of liver cancer.

Discussion

Arsenic trioxide has been demonstrated to be an effective

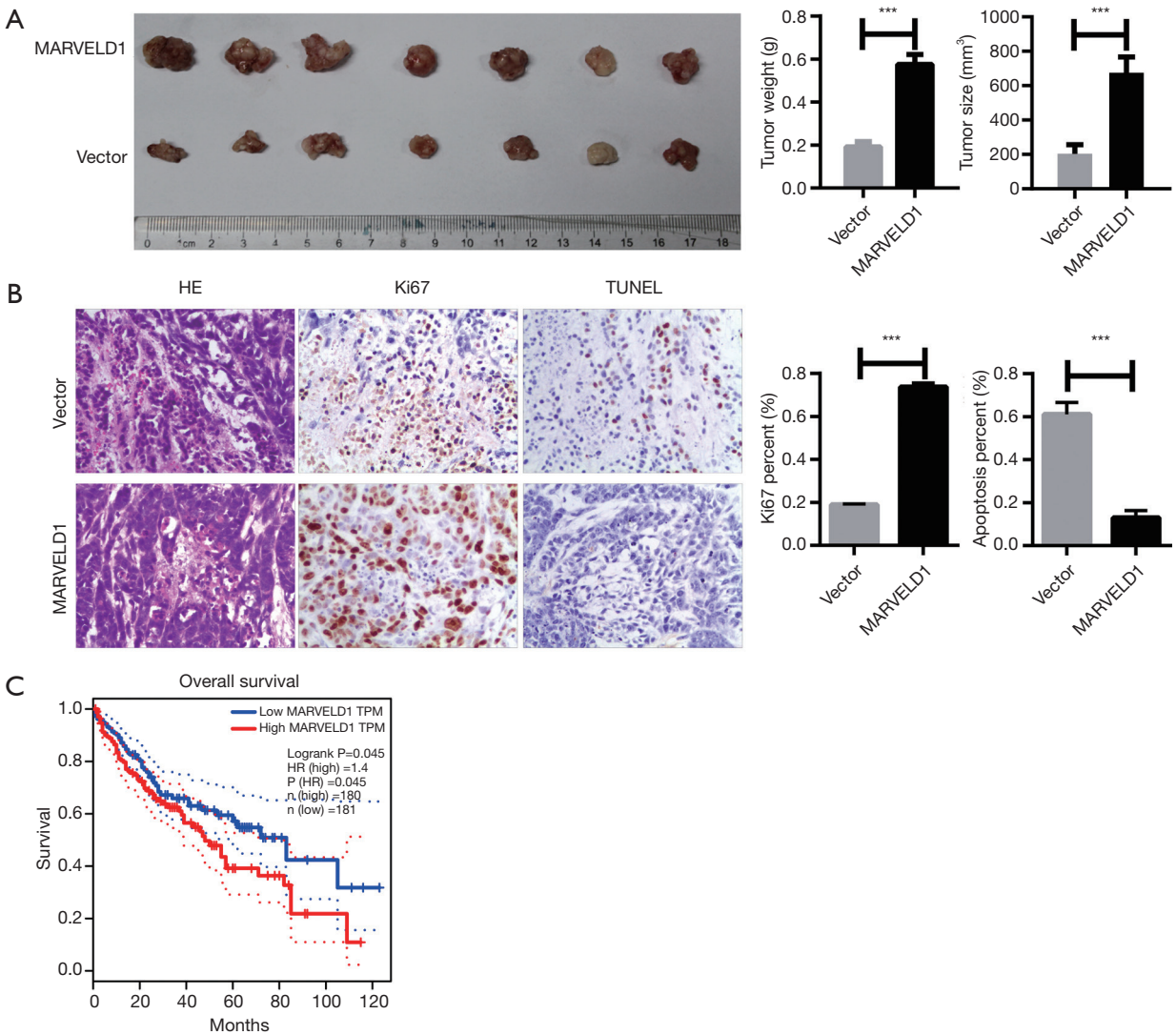

Figure 4 MARVELD1 induces resistance of liver cancer cells to As_2O_3 *in vivo*. (A) Left, representative images of tumors formed by HepG2-MARVELD1 stable cells and control cells in nude mice treated with As_2O_3; right, comparison of tumor weight and size between groups. (B) Left, HE and immunohistochemical staining of Ki67 and TUNEL assay of tumor tissue; right, quantification of Ki67 signal and DNA fragments. (C) Comparison of overall survival of liver cancer patients with high and low expression of MARVELD1 analyzed by GEPIA database tool. Data were pooled from at least two independent experiments. ***, P<0.001.

anti-cancer drug which induces complete remissions against APL (25). Moreover, arsenic trioxide also has great potential for the treatment of solid tumors. Drug resistance is one of the key obstacles for the effectiveness of drugs on recurrent cases of HCC. Arsenic trioxide has been proven to be a satisfactory inhibitor that can promote apoptosis and reduce migration inhibit invasion in HCC (26). A meta-analysis study revealed that adjuvant arsenic trioxide therapy combined with TACE achieves better therapeutic effects compared with TACE alone for higher therapeutic effects and lower toxic side effects (27). Advanced techniques may be used to improve the antitumor effects of As_2O_3. Chi *et al.* found that nanoparticle-loaded As_2O_3 had superior antitumor effects *in vivo* and *in vitro* compared to traditional free As_2O_3 and could induce more apoptotic cells in HCC (28).

Tyrosine kinase inhibitors (TKIs) can prevent the activation of signal pathways of growth and angiogenesis, and their treatment effects for HCC have gone through

tremendous changes. Several TKIs are applied to treat liver cancer, like sorafenib, sunitinib, and imatinib. TKIs can reduce the incidence rate of extrahepatic spread (EHS) and vascular invasion. Like traditional chemotherapy, TKIs also have been observed to have adverse reactions such as weakness, diarrhea, hypertension, arteriovenous thrombosis, hand-foot skin reactions, hemorrhage, etc. (29,30). Recently, Wang *et al.* reported that the combination of As_2O_3 and sorafenib demonstrated potential as a treatment in HCC cells for improved anti-tumor advantage and minimized toxicity (31). This suggests that the application of As_2O_3 may improve the TKI treatment effect on liver cancers.

The etiologies of HCC include a multitude of factors, such as virus type, gene mutation, alcohol, tumor microenvironment, along with other factors, all which lead to different pathological outcomes in HCC (32). HBV initiates the process of hepatic carcinogenesis by integrating into the host genome. Unlike HBV, HCV is an RNA virus that does not integrate its genomic material into the host genome. HCV carcinogenesis is mediated by the viral-induced factors and host-induced immunologic response. Alcohol-associated HCC occurs due to the metabolic process of alcohol inducing chronic oxidative stress leading to cirrhosis and eventually, malignancy. In NAFLD-associated HCC patients, the alteration of the gut microbiome was detected, and genetic polymorphisms were also found to be associated with the carcinogenesis. The different etiologies might activate common or specific pathways, and could provide clues for precision therapy of liver cancer in the future.

There is no evidence of an HBV genome in the HepG2 cell line (33). Some multidrug resistant proteins, such as ABCB1, ABCC1, and ABCC2 were associated with resistance in the selected arsenic trioxide resistant HepG2 cells. The expression of p53, MDM2, Gankyrin, and p-Rb also showed a significant increase in this system (34). Another study was carried out to identify molecular determinants for sensitivity and resistance of tumor cells towards arsenic trioxide by using microarray-based mRNA expression data in the NCI cell line panel. Twelve transcripts were identified to be associated with arsenic trioxide resistance in this study, including DNA biosynthesis and transcriptional regulation genes *(UPRT*, *MED12*, *SFRS15*) and the signal transduction gene, *ARHGEF6* (35).

MARVELD1 was identified as a potential tumor suppressor gene which could enhance the chemosensitivity of HCC cells to epirubicin and 10-hydroxycamptothecin. Interestingly, our results showed that MARVELD1 might contribute to arsenic trioxide resistance of the HCC cells by inhibiting apoptosis. It is commonly believed that As_2O_3 exerts its cytotoxic effect by increasing the intracellular ROS concentrations and inducing cell apoptosis (21). ROS induces depolarization of the mitochondria membrane and activation of the downstream caspase-dependent apoptosis pathways, such as caspase-3, caspase-8, and caspase-9 (36,37). In our study, we found that ROS induction was significantly suppressed by MARVELD1 overexpression. Arsenic can directly bind to thioredoxin reductase to alter the cellular redox state via its sulfur selenium group and inhibit its activity (23). Our results showed that overexpression of MARVELD1 could significantly increase the expression of thioredoxin reductase, resulting in the more effective elimination of ROS and reduced apoptosis *in vitro*. However, further perspective *in vivo* studies needs to be carried out to provide more evidence to prove this mechanism.

In conclusion, our study showed that overexpression of MARVELD1 could attenuate HCC cell apoptosis in response to As_2O_3 treatment by promoting thioredoxin reductase expression and effective elimination of ROS. Although more extensive work should be done to fully understand the role of MARVELD1 in cancer therapy, our study indicates that MARVELD1 may play an important role in predicting the prognosis of HCC patients treated with As_2O_3.

Acknowledgements

Funding: This work was supported by the National Natural Sciences Foundation of China (No. 81672321) and the clinical scientific research by the General Hospital of the PLA (2015FC-CXYY-3044).

Footnote

Conflicts of Interest: The authors have no conflicts of interest to declare.

Ethical Statement: All procedures followed the Peking University Guidelines for using animals in intramural research and were approved by the Animal Care and Use Committee of Peking University (No. LA2013-46).

References

1. El-Serag HB, KL Rudolph. Hepatocellular carcinoma: epidemiology and molecular carcinogenesis. Gastroenterology 2007;132:2557-76.
2. Daher S, Massarwa M, Benson AA, et al. Current and Future Treatment of Hepatocellular Carcinoma: An Updated Comprehensive Review. J Clin Transl Hepatol 2018;6:69-78.
3. Balogh J, Victor D 3rd, Asham EH, et al. Hepatocellular carcinoma: a review. J Hepatocell Carcinoma 2016;3:41-53.
4. Agni RM. Diagnostic histopathology of hepatocellular carcinoma: A case-based review. Semin Diagn Pathol 2017;34:126-37.
5. Xu N, Zhang J, Shen C, et al. Cisplatin-induced downregulation of miR-199a-5p increases drug resistance by activating autophagy in HCC cell. Biochem Biophys Res Commun 2012;423:826-31.
6. Beauchamp EM, Uren A. A new era for an ancient drug: arsenic trioxide and Hedgehog signaling. Vitam Horm 2012;88:333-54.
7. Hoonjan M, Jadhav V, Bhatt P. Arsenic trioxide: insights into its evolution to an anticancer agent. J Biol Inorg Chem 2018;23:313-29.
8. Zhang L, Liu L, Zhan S, et al. Arsenic Trioxide Suppressed Migration and Angiogenesis by Targeting FOXO3a in Gastric Cancer Cells. Int J Mol Sci 2018;19:19.
9. Zheng L, Jiang H, Zhang ZW, et al. Arsenic trioxide inhibits viability and induces apoptosis through reactivating the Wnt inhibitor secreted frizzled related protein-1 in prostate cancer cells. Onco Targets Ther 2016;9:885-94.
10. Li T, Cheng Y, Wang P, et al. CMTM4 is frequently downregulated and functions as a tumour suppressor in clear cell renal cell carcinoma. J Exp Clin Cancer Res 2015;34:122.
11. Yuan W, Liu B, Wang X, et al. CMTM3 decreases EGFR expression and EGF-mediated tumorigenicity by promoting Rab5 activity in gastric cancer. Cancer Lett 2017;386:77-86.
12. Wang S, Li Y, Han F, et al. Identification and characterization of MARVELD1, a novel nuclear protein that is down-regulated in multiple cancers and silenced by DNA methylation. Cancer Lett 2009;282:77-86.
13. Yu Y, Zhang Y, Hu J, et al. MARVELD1 inhibited cell proliferation and enhance chemosensitivity via increasing expression of p53 and p16 in hepatocellular carcinoma. Cancer Sci 2012;103:716-22.
14. Vermes I, Haanen C, Steffens-Nakken H, et al. A novel assay for apoptosis. Flow cytometric detection of phosphatidylserine expression on early apoptotic cells using fluorescein labelled Annexin V. J Immunol Methods 1995;184:39-51.
15. Rieger AM, Nelson KL, Konowalchuk JD, et al. Modified annexin V/propidium iodide apoptosis assay for accurate assessment of cell death. J Vis Exp 2011;50:15.
16. Ly JD, Grubb DR, Lawen A. The mitochondrial membrane potential (deltapsi(m)) in apoptosis; an update. Apoptosis 2003;8:115-28.
17. Matassov D, Kagan T, Leblanc J, et al. Measurement of apoptosis by DNA fragmentation. Methods Mol Biol 2004;282:1-17.
18. Errami Y, Naura AS, Kim H, et al. Apoptotic DNA fragmentation may be a cooperative activity between caspase-activated deoxyribonuclease and the poly(ADP-ribose) polymerase-regulated DNAS1L3, an endoplasmic reticulum-localized endonuclease that translocates to the nucleus during apoptosis. J Biol Chem 2013;288:3460-8.
19. Arora S, Tandon S. DNA fragmentation and cell cycle arrest: a hallmark of apoptosis induced by Ruta graveolens in human colon cancer cells. Homeopathy 2015;104:36-47.
20. Zhao X, Gao S, Ren H, et al. Inhibition of autophagy strengthens celastrol-induced apoptosis in human pancreatic cancer in vitro and in vivo models. Curr Mol Med 2014;14:555-63.
21. Selvaraj V, Armistead MY, Cohenford M, et al. Arsenic trioxide (As(2)O(3)) induces apoptosis and necrosis mediated cell death through mitochondrial membrane potential damage and elevated production of reactive oxygen species in PLHC-1 fish cell line. Chemosphere 2013;90:1201-9.
22. Lillig CH, Holmgren A. Thioredoxin and related molecules--from biology to health and disease. Antioxid Redox Signal 2007;9:25-47.
23. Lu J, Chew EH, Holmgren A. Targeting thioredoxin reductase is a basis for cancer therapy by arsenic trioxide. Proc Natl Acad Sci U S A 2007;104:12288-93.
24. Tang Z, Li C, Kang B, et al. GEPIA: a web server for cancer and normal gene expression profiling and interactive analyses. Nucleic Acids Res 2017;45:W98-102.
25. Coombs CC, Tavakkoli M, Tallman MS. Acute promyelocytic leukemia: where did we start, where are we now, and the future. Blood Cancer J 2015,5:e304.
26. Sadaf N, Kumar N, Ali M, et al. Arsenic trioxide induces apoptosis and inhibits the growth of human liver cancer cells. Life Sci 2018,205:9-17.
27. Lv XH, Wang CH, Xie Y. Arsenic trioxide combined with

transarterial chemoembolization for primary liver cancer: A meta-analysis. J Gastroenterol Hepatol 2017;32:1540-7.
28. Chi X, Zhang R, Zhao T, et al. Targeted arsenite-loaded magnetic multifunctional nanoparticles for treatment of hepatocellular carcinoma. Nanotechnology 2019;30:175101.
29. Nishida N, Kudo M. Immune checkpoint blockade for the treatment of human hepatocellular carcinoma. Hepatol Res 2018;48:622-34.
30. Kudo M. Systemic Therapy for Hepatocellular Carcinoma: Latest Advances. Cancers (Basel) 2018;10:11.
31. Wang L, Min Z, Wang X, et al. Arsenic trioxide and sorafenib combination therapy for human hepatocellular carcinoma functions via up-regulation of TNF-related apoptosis-inducing ligand. Oncol Lett 2018;16:3341-50.
32. Ghouri YA, Mian I, Rowe JH. Review of hepatocellular carcinoma: Epidemiology, etiology, and carcinogenesis. J Carcinog 2017;16:1.
33. Knowles BB, Howe CC, Aden DP. Human hepatocellular carcinoma cell lines secrete the major plasma proteins and hepatitis B surface antigen. Science 1980;209:497-9.
34. Chen X, Zhang M, Liu LX. The overexpression of multidrug resistance-associated proteins and gankyrin contribute to arsenic trioxide resistance in liver and gastric cancer cells. Oncol Rep 2009;22:73-80.
35. Sertel S, Tome M, Briehl MM, et al. Factors determining sensitivity and resistance of tumor cells to arsenic trioxide. PLoS One 2012;7:e35584.
36. Chen W, Martindale JL, Holbrook NJ, et al. Tumor promoter arsenite activates extracellular signal-regulated kinase through a signaling pathway mediated by epidermal growth factor receptor and Shc. Mol Cell Biol 1998;18:5178-88.
37. Gupta S, Yel L, Kim D, et al. Arsenic trioxide induces apoptosis in peripheral blood T lymphocyte subsets by inducing oxidative stress: a role of Bcl-2. Mol Cancer Ther 2003;2:711-9.

Cite this article as: Ma W, Shen H, Li Q, Song H, Guo Y, Li F, Zhou X, Guo X, Shi J, Cui Q, Xing J, Deng J, Yu Y, Liu W, Zhao H. MARVELD1 attenuates arsenic trioxide-induced apoptosis in liver cancer cells by inhibiting reactive oxygen species production. Ann Transl Med 2019;7(9):200. doi: 10.21037/atm.2019.04.38

Supplementary

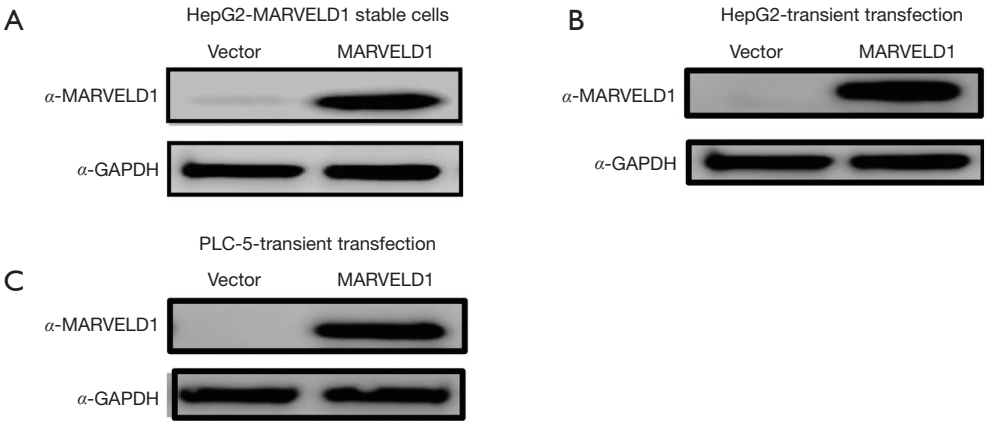

Figure S1 Confirmation of efficient expression of MARVELD1. (A). Immunoblotting of MARVELD1 in HepG2-MARVELD1 stable cells. (B) Immunoblotting of MARVELD1 in HepG2 cells transiently transfected with MARVELD1 plasmid. (C) Immunoblotting of MARVELD1 in PLC-5 cells transiently transfected with MARVELD1 plasmid.

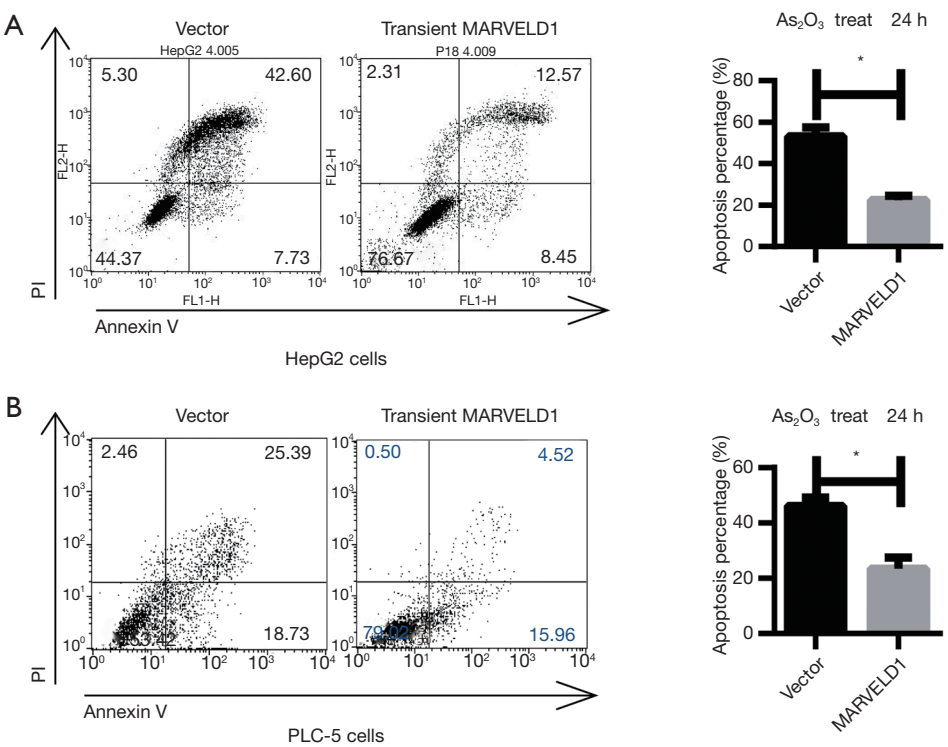

Figure S2 Overexpression of MARVELD1 inhibits apoptosis in HepG2 and PLC-5 cells treated with As_2O_3. (A) Flow cytometry analysis of apoptosis of HepG2 cells transiently transfected with MARVELD1 and control cells treated with As_2O_3 for 24 hours. (B) Flow cytometry analysis of apoptosis of PLC-5 cells transiently transfected with MARVELD1 and control cells treated with As_2O_3 for 24 hours. Data were pooled from at least three independent experiments. *, $P<0.05$.

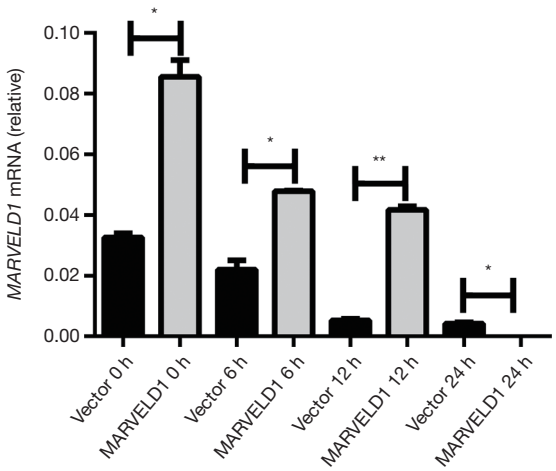

Figure S3 Time course of MARVELD1 mRNA level change. Time course of MARVELD1 mRNA level change in HepG2-MARVELD1 stable cells and control cells treated with As_2O_3. Data were pooled from at least three independent experiments. *, P<0.05. **, P<0.01.

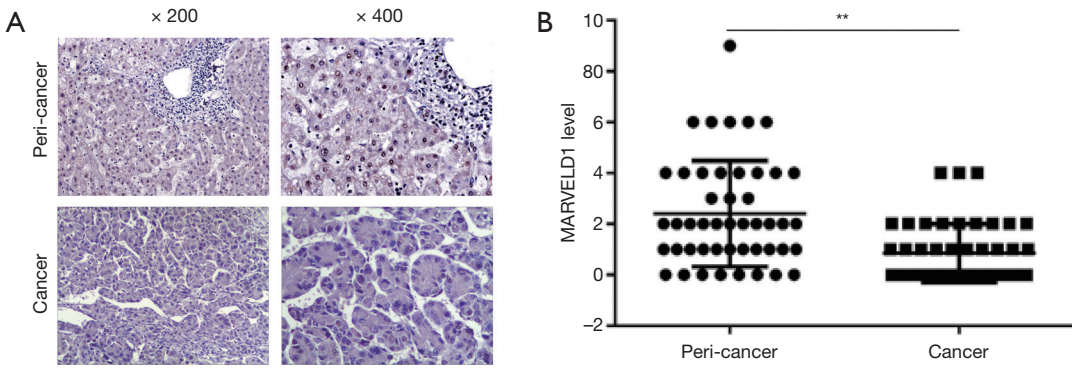

Figure S4 Immunohistochemical analysis of MARVELD1 expression in benign HCC tissues and peri-cancer tissues. (A) Representative images of MARVELD1 expression in HCC and peri-cancer tissues picked from different stages of HCC by IHC (×200, ×400). (B) The statistical results of the difference of MARVELD1 expression in HCC and peri-carcinomatous tissue analyzed by paired *t*-test. n=47. P<0.01. Data were pooled from at least two independent experiments. **, P<0.01.